www.czasopisma.pan.pl PAN www.journals.pan.pl
Metrol. Meas. Syst., Vol. 27 (2020) No. 4, pp. 659–672
DOI: 10.24425/mms.2020.134845

PAN POLSKA AKADEMIA NAUK
METROLOGY AND MEASUREMENT SYSTEMS
Index 330930, ISSN 0860-8229
www.metrology.wat.edu.pl
M&MS

AN ASSESSMENT OF APPLICABILITY OF THE TWO-DIMENSIONAL WAVELET TRANSFORM TO ASSESS THE MINIMUM CHIP THICKNESS DETERMINATION ACCURACY

Damian Gogolewski, Włodzimierz Makieła, Łukasz Nowakowski

Kielce University of Technology, Faculty of Mechatronics and Mechanical Engineering, al. 1000-lecia P.P. 7, 25-314 Kielce, Poland (✉ *dgogolewski@tu.kielce.pl*, +48 413 424 453, *wmakiela@tu.kielce.pl*, *lukasn@tu.kielce.pl*)

Abstract

The objective of the study was to assess the potential use of optical measuring instruments to determine the minimum chip thickness in face milling. Images of scanned surfaces were analyzed using mother wavelets. Filtration of optical signals helped identify the characteristic zones observed on the workpiece surface at the beginning of the cutting process. The measurement data were analyzed statistically. The results were then used to estimate how accurate each measuring system was to determine the minimum uncut chip thickness. Also, experimental verification was carried out for each mother wavelet to assess their suitability for analyzing surface images.

Keywords: Wavelet analysis, face milling, minimum chip thickness, surface texture.

Nomenclature

A	stagnation point
MA	method accuracy
a_p	axial depth of cut, µm
bior3.1	mother wavelet Biorthogonal of order 3.1
bior4.4	mother wavelet Biorthogonal of order 4.4
bior6.8	mother wavelet Biorthogonal of order 6.8
coif5	mother wavelet Coiflet of order 5
db10	mother wavelet Daubechies of order 10
db20	mother wavelet Daubechies of order 20
f_z	feed rate, mm/tooth
h_i	minimum chip thickness determined for selected sample, µm
$h_{\min}$	minimum chip thickness, µm
h_{ref}	reference value, µm
n	spindle speed, rpm
r_n	edge radius, °
s	standard deviation
sym10	mother wavelet Symlet of order 10
v_c	cutting speed, m/min
v_f	feed rate, mm/min
α	rake angle, °
β	inclination angle, °
θ	stagnation angle, °
φ	low-pass filter
ψ	high-pass filter
ψ^d	diagonal details signal
ψ^h	horizontal details signal
ψ^v	vertical details signal

1. Introduction

The quality of machine parts is largely dependent on the degree to which dimensional and geometrical requirements have been met and whether the desired surface texture has been achieved. Since surface condition is generally attributable to roughing and finishing operations, it is important that the right process parameters be first selected and then maintained [1].

When the milling operation requires the chip thickness to be smaller than the cutting edge radius, one of the key parameters to be determined is the minimum uncut thickness, which is a critical value defining the moment at which the material separated, *i.e*. removed, from the parent work material takes the form of a full chip. The analysis of the workpiece surface shows that there are three zones differing in the effect of the cutting tool, all dependent on the depth of cut. The first is the zone where there are only elastic-plastic deformations caused by the rubbing of the tool against the workpiece surface. In this case, the depth of cut is smaller than the smallest amount of material removable ($a_p < h_{\min}$). The next is the zone of elastic-plastic deformations where the material is partially removed ($a_p \approx h_{\min}$). The third is the zone in which the material is removed in the form of full chips ($a_p > h_{\min}$).

From a review of the literature it is apparent that the methods used to determine $h_{\min}$ fall into two groups:

– theoretical methods, based on formulae that take account of the cutting tool geometry and the workpiece material properties,
– experimental methods, which require measurement with specialist equipment.

The authors of this paper have recently been studying the potential use of the two-dimensional wavelet transform for this purpose. The novelty is a complex analysis of the influence of the mother wavelet on images of scanned surfaces filtration. In the paper were examined surface images obtained using selected optical measuring instruments. In particular images, the zone of initiating the face milling process was presented. Moreover, the results were compared with theoretical values determined based on theoretical formulas.

In the literature, the minimum chip thickness is generally defined in relation to cutting edge radius r_n. This relationship, however, is dependent on rake angle α, stagnation angle θ and axial depth of cut a_p [2].

The diagram in Fig. 1 illustrates the plastic flow of material along the cutting edge with radius r_n. Stagnation point A divides the flow into two zones: one above and the other below. The material that is below the point flows downwards from the cutting edge but no chips are formed.

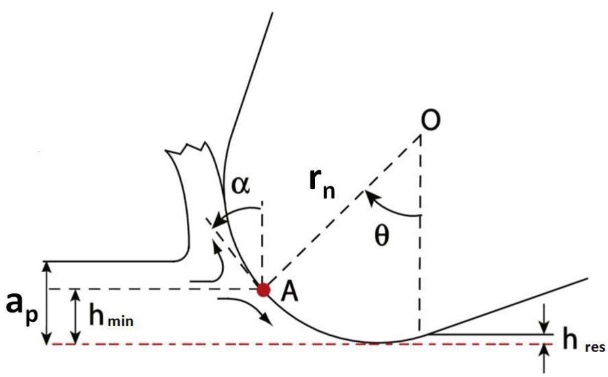

Fig. 1. Material flow along the rounded cutting edge.

This phenomenon is called ploughing; elastic-plastic deformations occur, but there is no material removal. Above the stagnation point, however, the material flows upwards and is removed in the form of chips. The position of the stagnation point at the edge radius is defined by stagnation angle θ. Stagnation angle θ and negative effective rake angle α (where $\alpha = \pi/2 - \theta$) are used to determine the minimum chip thickness, and this relationship can be written as:

$$h_{\min} = r_n(1 - \cos\theta). \tag{1}$$

There are numerous studies dealing with the effect of the negative rake angle on the minimum chip thickness in cutting. Sedriks and Mulhearn [3] indicate that the rake angle is mainly dependent on the coefficient of friction between the surfaces in contact, *i.e.*, the tool and the workpiece. In [4], Kita *et al.* discuss changes in the stagnation area, dependent both on the cutting speed and the properties of the workpiece material. If the minimum chip thickness is to be determined using relationship (1), it is necessary to know stagnation angle θ. L'vov [5] reported stagnation angle θ to be 45°, which gives $h_{\min} = 0.29r_n$. Basurar *et al.* [6] assume stagnation angle θ to reach 37.6°, thus, $h_{\min} = 0.21r_n$. Yuan *et al.* [7] show that minimum chip thickness $h_{\min}$ determined for aluminum alloys ranges from $0.25r_n$ to $0.32r_n$. From the numerical model developed by Ducobuet *et al.* [8], it is evident that when $h_{\min} \leq 0.25r_n$, no chip formation takes place.

Kawalec [9] suggests that the minimum chip thickness should be calculated taking into consideration the coefficient of proportionality k, dependent on the friction between the tool and the workpiece. Coefficient k can range from 0.1 to 1

$$h_{\min} = kr_n. \tag{2}$$

There are various models to determine the value of parameter $h_{\min}$. Some require a molecular and mechanical approach to dry friction as in Grzesik [10], others, for example, that proposed by Blake and Scattergood [11], take account of the fracture toughness, modulus of elasticity and Knoop hardness of the workpiece material. Their model is used to determine the critical value of parameter $h_{\min}$.

From the analysis of the methods and formulae for determining the minimum uncut chip thickness, it is clear that most of them are based on the cutting edge radius, which is multiplied by coefficient k ranging theoretically between 0.1 and 1. There are models that require knowledge of many complex relationships or experimentally determined constants. The proposed relationships, however, allow us to calculate only the critical values without defining their variability according to the cutting conditions and the workpiece material.

With the developments in science and technology, it has been essential to look for alternative solutions to facilitate the manufacturing of machine parts as well as improve equipment for their inspection, which may require filtration and analysis of measuring signals [12, 13]. The advances in numerical control and computer science have contributed to more complex but also more accurate measuring systems, capable of acquiring and processing large sets of data, *i.e.* signals. Systems with high computing efficiency are able to apply complex calculation models. Classical methods for the analysis of measuring signals are now being replaced with sophisticated data processing algorithms, which help better understand actual phenomena occurring during machining. These phenomena should be treated as unsteady state signals which need to be handled with proper equipment. The wavelet transform, developed at the turn of the 21st century, seems suitable for signal analysis. As it can be used to analyze signals with non-periodic irregularities and determine the place of their occurrence, the wavelet transform is becoming increasingly popular in many fields of science.

The concept of discrete wavelet transform is based on two mutually complementary high-pass (ψ) and low-pass (φ) filters in the x and y directions. Thus, surface analysis involves decomposing a measuring signal into four further signals ($i.e.$ the approximated signal and the signals of the horizontal, vertical and diagonal details). The approximated signal corresponds to low-frequency information, while the details are high-frequency information in the particular directions.

$$\varphi(x, y) = \varphi(x)\varphi(y), \tag{3}$$

$$\psi^{v}(x, y) = \psi(x)\varphi(y), \tag{4}$$

$$\psi^{h}(x, y) = \varphi(x)\psi(y), \tag{5}$$

$$\psi^{d}(x, y) = \psi(x)\psi(y). \tag{6}$$

Unlike the classical methods for the analysis of measuring signals, the wavelet transform can use a variety of mother wavelets. Each group of wavelets has some characteristic properties and the selection of an appropriate mother wavelet is very important for the analysis [14].

Wavelet transforms are commonly used in surface metrology [14–32]. Their applications include surface characterization [15, 16], especially for quality inspection purposes [17-20], which may require surface texture separation into roughness, waviness and form [21, 22]. The literature shows that multiscale analysis can be employed, for instance, to assess the wear of orthopedic implants [23] or the flank surface of the cutting tool [24]; it is also useful to study the effect of abrasive finishing on the surface texture [25], or to analyze the effects of different machining processes on the leak tightness of seals [26]. Jiang *et al.* [27] discuss the use of wavelet analysis to assess surface texture features for engineering and biomedical applications. Abdul-Rahman *et al.* [28] deal with freeform surfaces, while Stępień [29] investigates surface irregularities of cylindrical objects. The use of empirical mode decomposition to study surface topography is discussed by Zhang *et al.* [30]. As shown in [31, 32], mother wavelets can be employed to analyze 2D and 3D surface profiles in order to detect characteristic features or indicate their position from the signal. This suggests that wavelet analysis is suitable for determining the length of the zones where the cutting is initiated.

2. Materials and methods

The experiments were divided into two stages. First, milling was performed on ten specimens. Then, the machined surfaces were analyzed to identify the characteristic zones, corresponding to the different effects of the tool on the workpiece material. The milling was initiated gradually on C45 steel specimens (Fig. 2) with no cutting fluid present. The operation was carried out using a DMG MORI DMU 50 universal milling machine. The specimens used for the tests were octagonal in cross-section, which made them easy to secure in a vice. Because of their shape, $i.e.$ four pairs of parallel sides, the specimens were easy to fix in a four-jaw chuck and measure using different equipment with no special clamps. The tool was a Sandvik Coromant CoroMill 490 milling cutter with a 490–08T308M–PL sintered carbide insert where the cutting edge radius r_n was 56 µm. The expanded uncertainty of measurement of the edge radius was equal ±1 µm (probability 95%, k = level 2). Applying one insert only allowed us to eliminate axial and/or radial runout which could have affected the measurement results. Gradual initiation of the cutting process was possible by inclining the milled surface to achieve gradual immersion of the cutter, which moved parallelly to the table surface. The surface to be milled was polished to obtain roughness at least one order lower than that achieved through milling for easier identification of

Metrol. Meas. Syst., Vol. 27 (2020), No. 4, pp. 659–672
DOI: 10.24425/mms.2020.134845

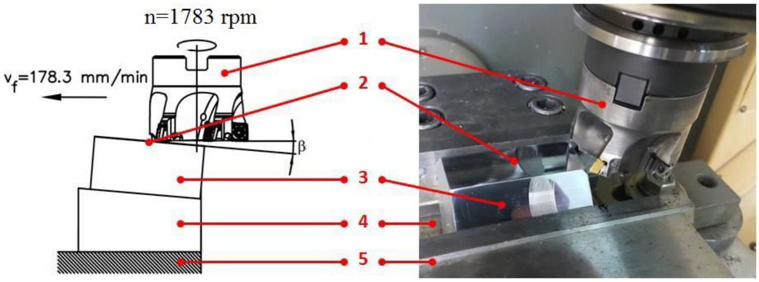

Fig. 2. View of the milling process. 1 – tool, 2 – surface to be cut, 3 – workpiece, 4 – wedge, 5 – machine vice, v_f – feed rate, n – spindle speed, β – inclination angle.

the characteristic zones. Flatness measurements were necessary to determine the polishing errors (Table 1), and these were carried out using a PRISMO Navigator coordinate measuring machine equipped with a VAST GOLD S-ACC active scanning and multi-point sensor. The measurement data indicated that the rounded workpiece edges being a result of polishing (Fig. 3) had no effect on the surface to be cut. The surface flatness error measured for the ten specimens ranged from 0.011 to 0.018 mm (Table 1).

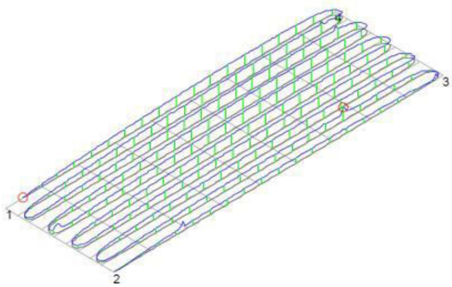

Fig. 3. Flatness analysis for Specimen No. 5.

Table 1. Surface flatness recorded for the specimens tested.

Specimen number	1	2	3	4	5	6	7	8	9	10
Surface flatness, mm	0.011	0.013	0.014	0.016	0.010	0.011	0.011	0.018	0.017	0.016

The next stage of the experiments consisted in placing the specimens on a wedge with an inclination angle β of $0°12'00''$. The specimen fixing is illustrated in Fig. 2. Before milling, the inclination angle was measured for each specimen using a Heidenhain TS 640 touch probe installed on the milling machine. The measurement results are given in Table 2.

Table 2. Inclination angle for each specimen milled.

Specimen number	1	2	3	4	5	6	7	8	9	10
Inclination angle	$0°11'$ $56''$	$0°11'$ $34''$	$0°10'$ $24''$	$0°10'$ $58''$	$0°13'$ $30''$	$0°12'$ $32''$	$0°12'$ $07''$	$0°13'$ $40''$	$0°12'$ $21''$	$0°10'$ $44''$

The ten specimens used in the experiment were milled at the same cutting speed (v_c = 280 m/min) and the same feed rate (f_z = 0.1 mm/tooth). The process parameters were selected following the recommendations of the insert producer and taking into consideration the properties of the workpiece material. The material tested, *i.e.* C45 carbon steel, can be thermally hardened which makes it difficult to weld but easy to machine. It exhibits a tendency to adhere to the cutting tool which leads to edge build-up. Because of poor machinability, rough surfaces are obtained. The steel is used for moderate load applications, including spindles, axles, crankshafts, unhardened gears, electric motor shafts, regular knives, corkscrews, wheel hubs, discs, rods, cylinders and pump impellers.

The final stage involved analyzing the surface images by means of the following mother wavelets: *db10, db20, coif5, sym10, bior3.1, bior4.4*, and *bior6.8*. For each wavelet, tests were carried out at several levels of decomposition. The images of approximated signals were analysed, as well as images of the detail signals obtained at particular levels. The research was carried out in a complex way by analyzing individual signals separately, as well as by adding individual images in different configurations to each other. This was possible because wavelet transformation allows to reconstruct signal at any time [29]. Moreover, the threshold method was used to emphasize particular zones. All performed procedures allowed to expose the key features of the signal.

The images used to identify the zone where the machining process was initiated were obtained by applying three optical measuring instruments (Fig. 4). Providing high resolution in each measurement axis, this equipment can be used in specialist laboratories as well as under industrial conditions. The use of different types of measuring systems helped assess the effect of their resolution on $h_{\min}$. It was vital to determine what experimental accuracy each vision system offered when the minimum chip thickness was determined. This allowed to examine whether instruments with not very high resolution of particular axes can be used to determine the key parameters of the face milling process.

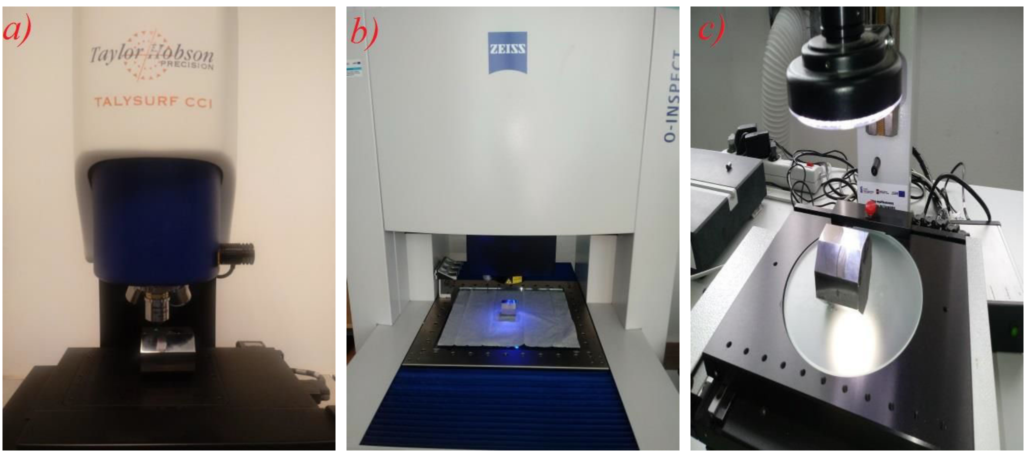

Fig. 4. (a) Talysurf CCI Lite, (b) O-Inspect 442 multi-sensor measuring machine, (c) MarVision MM 320 workshop microscope.

The equipment used for the measurements can be characterized as follows.

– The Taylor Hobson Talysurf CCI Lite is a non-contact optical system designed to measure surface texture using a vertical resolution of the order of 0.01 nm and a horizontal resolution of the order of 0.33 µm. The measurement system is based on *coherence correlation*

interferometry (CCI). It employs pneumatic vibration isolators to offer ultra-precision. The software is capable of stitching several scanned images together.
– The ZEISS O-Inspect 442 multi-sensor measuring machine is an optical system equipped with a Discovery V12 varifocal zoom lens providing a magnification of up to ×12. The system measuring range is 400 × 400 × 200 mm, with the length measurement error being 1.7 + $L/250$ µm.
– The MarVision MM 320 workshop measuring microscope has an XY stage travel range of 200 × 100 mm, a resolution of 0.001 mm and a maximum error of 3 + $L/100$ µm. Its features include a zoom lens offering a magnification of ×0.7 up to ×4.5 and dimmable a LED transmitted light.

3. Results

The study consisted in scanning the specimen surfaces after the milling process. The measurements were taken using the Talysurf CCI optical profiler, the O-Inspect 442 multi-sensor measuring machine and the MarVision MM320 workshop microscope (at a magnification of ×0.7, ×1 or ×2). The reference value of the minimum chip thickness was assumed to be equal to the value determined on the basis of a set of measuring points obtained with the optical profiler. Examples of surface texture images recorded with the selected measuring systems are shown in Fig. 5.

The experimental method accuracy (*MA*) was assessed for each measuring system. The calculations were made using relationships (7) and (8) at a probability (P) of 0.95. For this value, parameter t was determined from Student's t-distribution tables. The value was 2.262.

$$w_h = \frac{h_i - h_{ref}}{h_{ref}} 100\%, \tag{7}$$

$$MA = |\overline{w_h} \pm ts|_{\max}, \tag{8}$$

where h_i – minimum chip thickness, h_{ref} – reference value, s – standard deviation.

This method can be used to assess the suitability of a measuring instrument for determining parameter $h_{\min}$. According to Adamczak *et al.* [33], the values obtained allow us to qualitatively and quantitatively estimate the parameter determination accuracy for any measuring system (Table 3).

Table 3. Relative error for surface texture measurement [33].

Measurement accuracy (%)	**Application**
2–5	measurement of reference standards: roughness, waviness, form profiles
5–15	research
10–25	industrial measurement of surface texture

The potential use of the selected measuring instruments was studied using the Talysurf CCI optical profiler as the reference system. It was essential to identify the area where the milling process was unstable. The minimum uncut chip thickness was determined using trigonometric functions while knowing the inclination angle of the wedge on which the specimen was placed. The value obtained was assumed to be the reference value. The theoretical values of parameter $h_{\min}$ were also calculated using the models available in the literature. These were then compared with

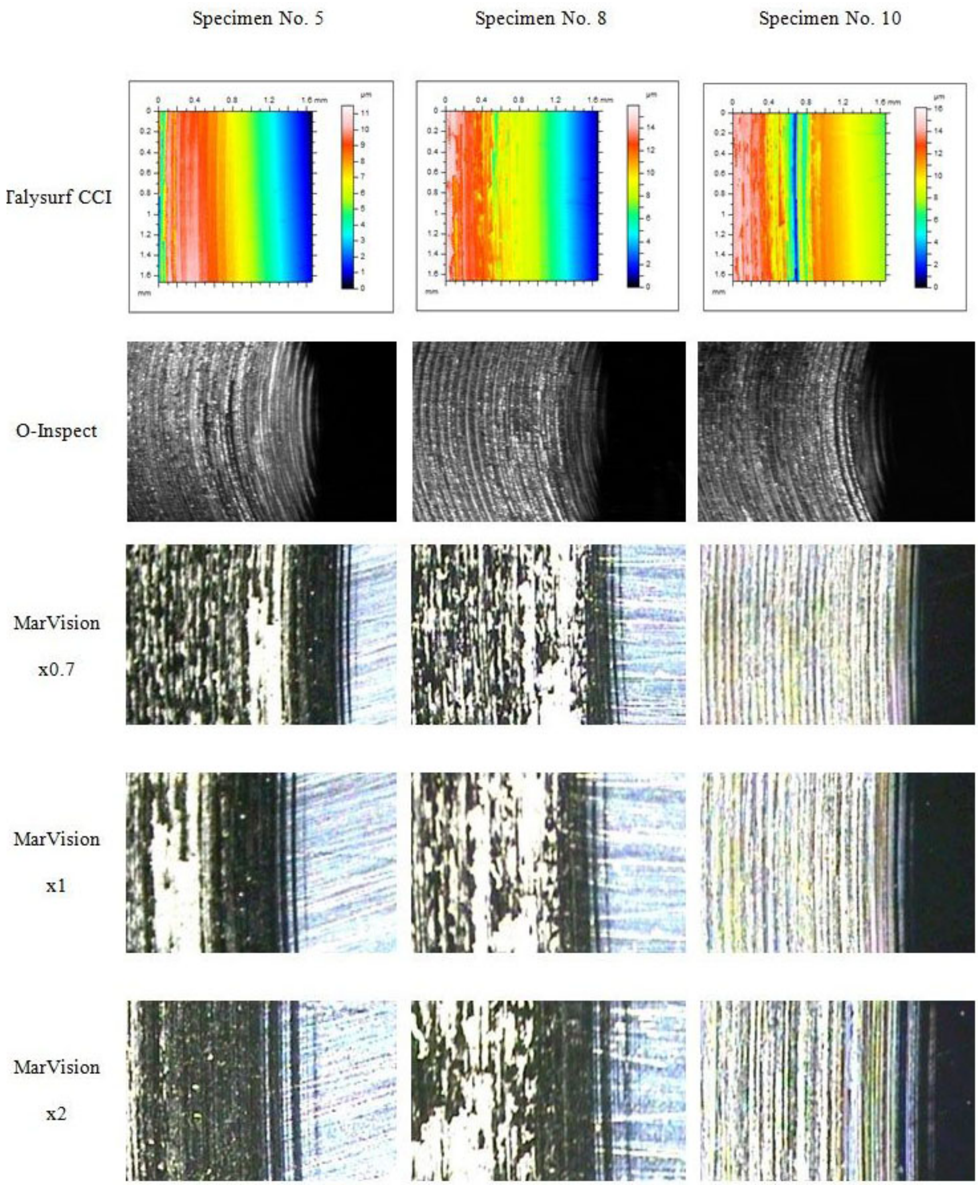

Fig. 5. Surface images obtained for specimens Nos. 5, 8 and 10 with the Talysurf CCI, the O-Inspect and the MarVision (magnified ×0.7, ×1 and ×2).

the experimental data. A review of the literature shows that the minimum chip thickness is strictly related to the cutting edge radius, *i.e.*, $h_{\min} = (0.21{-}0.32)r_n$. The theoretical value of parameter $h_{\min}$, calculated for a Sandvik Coromant CoroMill 490 milling cutter with a 490–08T308M–PL sintered carbide insert, where $r_n = 56$ µm, was: (0.21–0.32)56 = 11.76–17.92 µm.

The same procedure was employed to determine this parameter for all the measuring systems. However, the area where the milling process was initiated was identified by filtering the scanned images with the two-dimensional wavelet transform. The analysis involved filtering signal compo-

Metrol. Meas. Syst., Vol. 27 (2020), No. 4, pp. 659–672
DOI: 10.24425/mms.2020.134845

nents to precisely determine the characteristic milling zones (Figs. 6–10). The calculation results obtained by means of the *db10* mother wavelet are provided in Table 4.

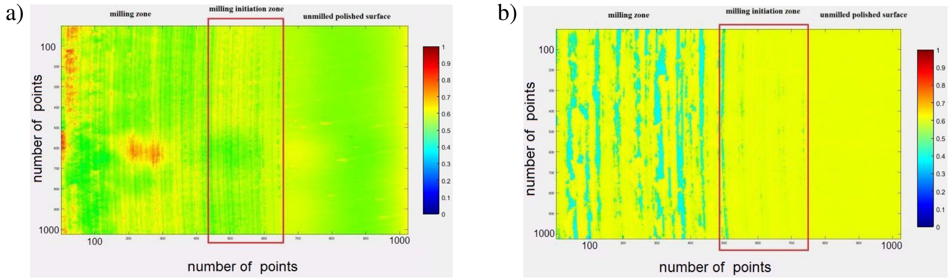

Fig. 6. Wavelet decomposition coefficients for surfaces scanned with the Talysurf CCI:
(a) Specimen No. 5, (b) Specimen No. 8.

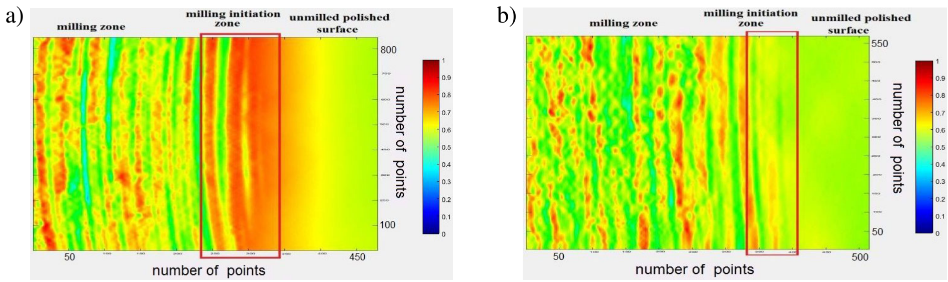

Fig. 7. Wavelet decomposition coefficients for surfaces scanned with the O-Inspect:
(a) Specimen No. 5, (b) Specimen No. 10.

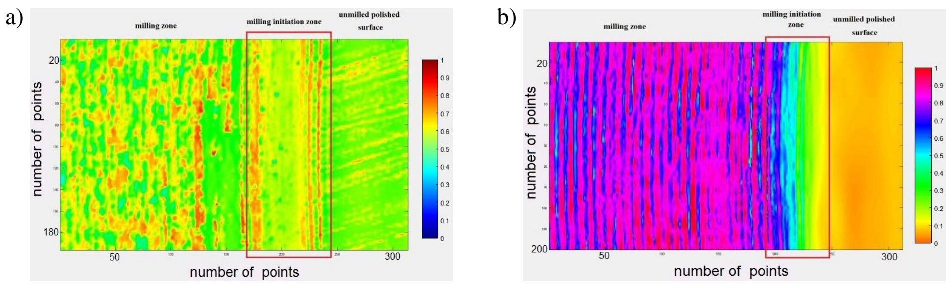

Fig. 8. Wavelet decomposition coefficients for surfaces scanned with the MarVision, magnification ×0.7:
(a) Specimen No. 5, (b) Specimen No. 10.

An analysis of the scanned surface images using the two-dimensional wavelet transform reveals that, despite the filtration of some surface roughness components, it is not possible to precisely map the areas differently affected by the cutter at the beginning of the milling operation. Such mapping requires special skills and knowledge. However, as can be seen from Table 4, the values of $h_{\min}$ calculated using the wavelet transform and those measured with the O-Inspect or the MarVision (×2) are only slightly different from the reference values determined on the basis of the measuring points provided by the Talysurf CCI optical profiler.

The analysis of the potential use of the three measuring machines to determine the minimum uncut chip thickness according to relationships (7) and (8) also included assessing the relative

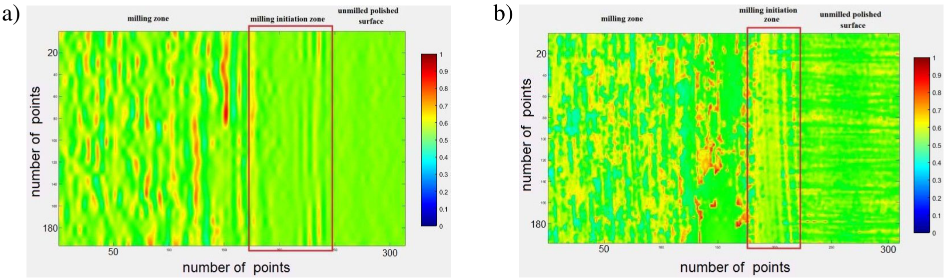

Fig. 9. Wavelet decomposition coefficients for surfaces scanned with the MarVision, magnification ×1: (a) Specimen No. 5, (b) Specimen No. 8.

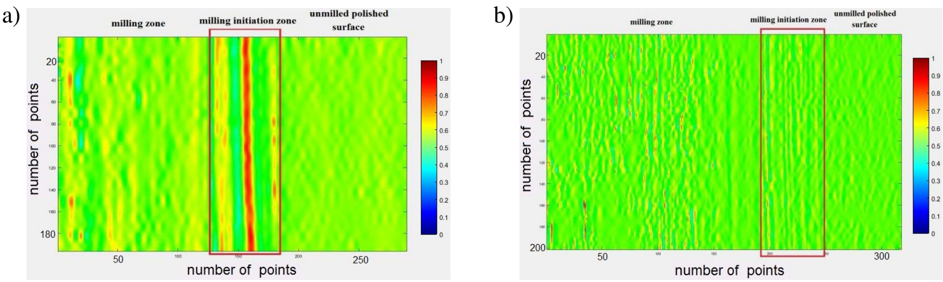

Fig. 10. Wavelet decomposition coefficients for surfaces scanned with the MarVision, magnification ×2: (a) Specimen No. 5, (b) Specimen No. 8.

Table 4. Minimum uncut chip thickness (filtration with the *db10* wavelet).

Specimen number	Theoretical model, μm	Talysurf CCI, μm		O-Inspect, μm	MarVision, μm		
	$h_{\min} = (0.21–0.32)r_n$	Reference value	Wavelet transform		×0.7	×1	×2
1	11.76–17.92	2.02	1.98	2.10	1.64	2.25	2.20
2		2.34	2.31	2.35	2.58	2.72	2.24
3		1.82	1.95	2.10	1.61	1.88	1.80
4		2.35	2.26	2.14	2.45	2.33	2.30
5		2.66	2.57	2.71	3.08	2.77	2.74
6		2.41	2.48	2.39	2.52	2.46	2.58
7		2.78	2.76	2.80	2.85	2.47	2.44
8		2.22	2.12	2.18	2.30	2.12	2.14
9		2.43	2.38	2.40	2.57	2.50	2.38
10		2.27	2.32	2.20	2.02	2.04	2.20

accuracy of a given method. The effect of the mother wavelet form on the filtration process was studied using different wavelet functions. The wavelets selected were: *db10, db20, coif5, sym10, bior3.1, bior4.4* and *bior6.8*. The values of the parameter defining the experimental accuracy of the method are given in Table 5.

The analysis shows that all the measuring instruments used in the experiments are well-suited for determining parameter $h_{\min}$. Its values ranged between 7.21% and 28.19%. From Table 3, it is evident that the method based on two-dimensional wavelet analysis can be used for research

Table 5. Experimental method accuracy, %.

Method accuracy, *MA*	Talysurf CCI	O-Inspect	MarVision		
			×0.7	×1	×2
MA (db10)	8.74	14.70	24.99	20.77	14.64
MA (db20)	9.08	11.28	28.19	18.33	13.08
MA (coif5)	8.44	13.86	20.16	18.75	14.35
MA (sym10)	8.63	13.41	26.71	18.26	11.25
MA (bior3.1)	9.14	14.26	25.15	18.76	15.60
MA (bior4.4)	7.23	13.64	23.76	20.89	14.49
MA (bior6.8)	7.21	12.85	24.66	18.34	12.80

applications. The most favorable results were reported for signals provided by the optical profiler. This is due to the high density of measuring points and accurate surface representation. The data provided by the O-Inspect multi-sensor measuring machine were also sufficient. The least satisfactory results were obtained with the MarVision workshop microscope. For a magnification of ×0.7 and ×1, parameter MA was above 15%. When the magnification was ×2, the method accuracy reported for the MarVision was the lowest. From Table 5, it is clear that the higher the magnification, the lower the values of the parameter. An exception is the value obtained in the analysis with the *bior3.1* mother wavelet.

4. Conclusions

Finish milling with small allowance requires knowledge of the minimum uncut chip thickness, *i.e.* the smallest thickness of material that can be removed under given cutting conditions. Determining this parameter using the currently available methods is a complex process. The measuring machine operator needs to have skills and experience to be able to properly interpret data in order to identify zones differing in the effect of the tool on the workpiece material. This study involved employing measuring instruments with high vertical and horizontal resolution and the two-dimensional wavelet transform to indicate the zones of the tool effect at the beginning of the cutting process. The images registered with the optical measuring instruments were decomposed using the two-dimensional wavelet transform. Separation of certain components helped locate the area where the actual cutting was initiated and, on this basis, determine the value of parameter $h_{\min}$.

The method accuracy MA was calculated for three measuring instruments to assess their suitability for determining the analyzed machining parameter so that such combined methods could be used for research applications. The lowest and therefore most favorable values of parameter MA were obtained for the Talysurf CCI optical profiler (MA: 7.21%–9.14%). The results reported for the O-Inspect 442 multi-sensor measuring machine were also low (MA: 11.28%–14.70%). It can be concluded that the two-dimensional wavelet transform is a well-suited tool to analyze surface images, for instance, to determine the minimum uncut chip thickness. The use of the wavelet analysis helped identify the different zones of the milling process initiation which were not clearly visible on the surface images before the wavelet filtration. In the case of the MarVision MM320 workshop microscope, it was also necessary to establish the degree to which the zone identification process was affected by the lens magnification. It was found that the higher the magnification, the smaller the value of parameter MA. However, the results obtained at the highest magnification tested show that this microscope can be used for determining the value of h_{min}. The findings show that the form of the mother wavelet had only a slight effect on the results. The minimum uncut chip thickness and the experimental method accuracy were reported to coincide for all the measuring instruments. The theoretical models to predict the minimum uncut chip thickness found in the literature assume that the parameter is highly dependent on the cutting edge radius and the relationship can be described as $h_{\mathrm{min}} = (0.21–0.32)r_n$. The modelling performed for a Sandvik CoroMill 490 milling cutter with a 490–08T308M–PL insert (r_n = 56 µm) revealed that the value of h_{min} was 5–7.7 times higher than that obtained experimentally. Because of these discrepancies, an alternative method was proposed to determine parameter h_{min}. As the experimental data show, the use of the wavelet analysis seems well suited for this purpose even in workshop instruments with not very high resolution of particular axes.

The developed method of surface filtration based on wavelet transformation made it possible to identify and precisely determine the length of the zones where the cutting is initiated. It allows to precisely assess the value of the minimum chip thickness which is an important parameter taken into account in the models for prediction of surface roughness and design of machining technology.

References

[1] Adamczak, S. & Zmarzły, P. (2019). Research of the influence of the 2D and 3D surface roughness parameters of bearing raceways on the vibration level. *Journal of Physics: Conference Series, 1183*, 012001. https://doi.org/10.1088/1742-6596/1183/1/012001

[2] Lee, K., & Dornfeld, D. A. (2005). Micro-burr formation and minimization through process control. *Precision Engineering, 29*(2), 246–252. https://doi.org/10.1016/j.precisioneng.2004.09.002

[3] Sedriks, A. J., & Mulhearn, T. O. (1964). The effect of work-hardening on the mechanics of cutting in simulated abrasive processes. *Wear, 7*(5), 451–459. https://doi.org/10.1016/0043-1648(64)90137-1

[4] Kita, Y., Ido, M., & Hata, S. (1978). The mechanism of metal removal by an abrasive tool. *Wear, 47*(1), 185–193. https://doi.org/10.1016/0043-1648(78)90214-4

[5] L'vov, N. P. (1969). Determining the minimum possible chip thickness. *Machines & Tooling, 4*, 40–45.

[6] Basuray, P. K., Misra, B. K., & Lal, G. K. (1977). Transition from ploughing to cutting during machining with blunt tools. *Wear, 43*(3), 341–349. https://doi.org/10.1016/0043-1648(77)90130-2

[7] Yuan, Z. J., Zhou, M., & Dong, S. (1996). Effect of diamond tool sharpness on minimum cutting thickness and cutting surface integrity in ultraprecision machining. *Journal of Materials Processing Technology, 62*(4), 327–330. https://doi.org/10.1016/S0924-0136(96)02429-6

[8] Ducobu, F., Filippi, E., & Rivière, L. (2009). Modélisation de l'influence de la profondeur de coupe en micro-coupe orthogonale. *19 Congrès Francais de Mécanique Marseille*. France. http://hdl.handle.net/2042/37240 (in French).

[9] Kawalec, M. (1980). *Fizyczne i technologiczne zagadnienia przy obróbce z małymi grubościami warstwy skrawanej*. [Rozprawy nr 106. Wydawnictwo Politechniki Poznańskiej]. (in Polish)

[10] Grzesik, W. (2010). *Podstawy skrawania materiałów konstrukcyjnych*. Wydawnictwa Naukowe PWN. (in Polish)

[11] Blake, P. N. & Scattergood, R. O. (1990). Ductile-regime machining of germanium and silicon. *Journal of the American ceramic society, 73*(4), 949–957. https://doi.org/10.1111/j.1151-2916.1990.tb05142.x

[12] Pawlus, P., Reizer, R., & Wieczorowski, M. (2018). Comparison of results of surface texture measurement obtained with stylus methods and optical methods. *Metrology and Measurement Systems, 25*(3), 589–602. https://doi.org/10.24425/123894

[13] Podulka, P. (2020). Comparisons of envelope morphological filtering methods and various regular algorithms for surface texture analysis. *Metrology and Measurement Systems, 27*(2), 243–263. https://doi.org/10.24425/mms.2020.132772

[14] Gogolewski, D. (2020). Influence of the edge effect on the wavelet analysis process, *Measurement, 152*, 107314. https://doi.org/10.1016/j.measurement.2019.107314

[15] Josso, B., Burton, D. R., & Lalor, M. J. (2002). Frequency normalised wavelet transform for surface roughness analysis and characterisation. *Wear, 252*(5-6), 491–500. https://doi.org/10.1016/S0043-1648(02)00006-6

[16] Brown, C. A., Hansen, H. N., Jiang, X., Blateyron, F., Berglund, J., Senin, N., Bartkowiak, T., Dixon, B., Le Goic, G., Quinsat, Y., Stemp, W. J., Thompson, M. K., Ungar, P. S., & Zahouani, H. (2018). Multiscale analyses and characterizations of surface topographies. *CIRP Annals – Manufacturing Technology, 67*(2), 839–862. https://doi.org/10.1016/j.cirp.2018.06.001

[17] Bruzzone, A. A. G., Montanaro, J. S., Ferrando, A., & Lonardo, P. M. (2004). Wavelet analysis for surface characterization: an experimental assessment. *CIRP Annals – Manufacturing Technology, 53*(1), 479–482. https://doi.org/10.1016/S0007-8506(07)60744-6

[18] Adamczak, S. & Makieła, W. (2011). Analyzing variations in roundness profile parameters during the wavelet decomposition process using the Matlab environment. *Metrology and Measurement Systems, 18*(1), 25–33. https://doi.org/10.2478/v10178-011-0003-6

[19] LeGoïc, G., Bigerelle, M., Samper, S., Favrelière, H., & Pillet, M. (2016). Multiscale roughness analysis of engineering surfaces: A comparison of methods for the investigation of functional correlations. *Mechanical Systems and Signal Processing, 66–67*, 437–457. https://doi.org/10.1016/j.ymssp.2015.05.029

[20] Zmarzły, P., Kozior, T., & Gogolewski, D. (2019). Dimensional and shape accuracy of foundry patterns fabricated through photo-curing. *Tehnički vjesnik – Technical Gazette, 26*(6), 1576–1584. https://doi.org/10.17559/TV-20181109115954

[21] Blateyron, F. (2014). Good practices for the use of areal filters, *Proceedings of 3rd Seminar on surface metrology of the Americas*, USA. https://doi.org/10.13140/2.1.1007.9361

[22] Gogolewski, D. & Makieła, W. (2019). Application of wavelet transform to determine surface texture constituents. In: Durakbasa N., & Gencyilmaz M. (Eds). *Proceedings of the International Symposium for Production Research 2018* (pp. 224–231). Springer. https://doi.org/10.1007/978-3-319-92267-6_19

[23] Jiang, X. Q. & Blunt, L. (2001). Morphological assessment of in vivo wear of orthopaedic implants using multiscalar wavelets. *Wear, 250*(1–12), 217–221. https://doi.org/10.1016/S0043-1648(01)00644-5

[24] Dutta, S., Pal, S. K., & Sen, R. (2016). Progressive tool flank wear monitoring by applying discrete wavelet transform on turned surface images. *Measurement, 77*, 388–401. https://doi.org/10.1016/j.measurement.2015.09.028

[25] Zahouani, H., Mezghani, S., Vargiolu, R., & Dursapt, M. (2008). Identification of manufacturing signature by 2D wavelet decomposition. *Wear, 264*(5–6), 480–485. https://doi.org/10.1016/j.wear.2006.08.047

[26] Deltombe, R., Bigerelle, M., & Jourani, A. (2015). Analysis of the effects of different machining processes on sealing using multiscale topography. *Surface Topography: Metrology and Properties, 4*(1). https://doi.org/10.1088/2051-672X/4/1/015003

[27] Jiang, X., Scott, P., & Whitehouse, D. (2008). Wavelets and their Applications for Surface Metrology. *CIRP Annals – Manufacturing Technology, 57*(1), 555–558. https://doi.org/10.1016/j.cirp.2008.03.110

[28] Abdul-Rahman, H. S., Jiang, X. J., & Scott, P. J. (2013). Freeform surface filtering using the lifting wavelet transform. *Precision Engineering, 37*(1), 187–202. https://doi.org/10.1016/j.precisioneng.2012.08.002

[29] Stępień, K. & Makieła, W. (2013). An analysis of deviations of cylindrical surfaces with the use of wavelet transform. *Metrology and Measurement Systems, 20*(1), 139–150. https://doi.org/10.2478/mms-2013-0013

[30] Zhang, Z., Zhang, Y., & Zhu, Y. (2010). A new approach to analysis of surface topography. *Precision Engineering, 34*(4), 807–810. https://doi.org/10.1016/j.precisioneng.2010.05.002

[31] Stępień, K. (2014). Research on a surface texture analysis by digital signal processing methods. *Tehnički vjesnik – Technical Gazette, 21*(3), 485–493.

[32] Gogolewski, D. (2018). The simulation method for the identification the surface irregularities. *24th International Conference Engineering Mechanics*, Czech Republic, 253–256. https://doi.org/10.21495/91-8-253

[33] Adamczak, S., Janusiewicz, A., Makieła, W., & Stępień, K. (2011). Statistical validation of the method for measuring radius variations of components on the machine tool. *Metrology and Measurement Systems, 17*(1), 35–46. https://doi.org/10.2478/v10178-011-0004-5

Damian Gogolewski received the Ph.D. degree in 2018. He is currently Assistant Professor at the Kielce University of Technology, Poland. His research activities focus on: surface metrology, multiscale analysis and characterizations, wavelet transformation and measurements of geometrical quantity.

Łukasz Nowakowski received the Ph.D. degree from Kielce University of Technology, in 2014. He is currently Assistant Professor with the Kielce University of Technology, Poland. He has authored or coauthored over 40 journal, 50 conference publications and 9 patents. His research activity focuses on machining processes, CAD/CAM systems, machine design.

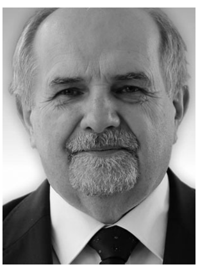

Włodzimierz Makieła (PhD, DSc), Professor at Kielce University of Technology, obtained 2 degrees: MCs Technical Engineer in Quantum Physics, AGH Kraków (1978), Mechanical Engineer, Kielce University of Technology (1991), he received post-doctoral dissertation (habilitation) at Technical University of Košice (2011); His research activities focus on: metrology of geometrical quantities, application of wavelet transformation in the evaluation of geometrical surface texture, accreditation and certification of quality assurance systems. He has authored & co-authored: 2 academic books, 60 articles & over 100 attestation research reports. He is currently Vice-rector for Science and Development at Kielce University of Technology.